

## Synthesis and Characterization of Open-Framework Niobium Silicates: $\text{Rb}_2(\text{Nb}_2\text{O}_4)(\text{Si}_2\text{O}_6) \cdot \text{H}_2\text{O}$ and the Dehydrated Phase $\text{Rb}_2(\text{Nb}_2\text{O}_4)(\text{Si}_2\text{O}_6)$

Jhen-Ming Tasi,<sup>†</sup> Po-Tao Tu,<sup>†</sup> Ting-Shan Chan,<sup>‡</sup> and Kwang-Hwa Lii<sup>\*,†,§</sup>

Department of Chemistry, National Central University, Zhongli, Taiwan, R.O.C., National Synchrotron Radiation Research Center, Hsinchu, Taiwan, R.O.C., and Institute of Chemistry, Academia Sinica, Taipei, Taiwan, R.O.C

Received August 11, 2008

A new niobium(V) silicate,  $\text{Rb}_2(\text{Nb}_2\text{O}_4)(\text{Si}_2\text{O}_6) \cdot \text{H}_2\text{O}$ , has been synthesized by a high-temperature, high-pressure hydrothermal method and characterized by single-crystal X-ray diffraction, thermogravimetric analysis, and solid-state NMR spectroscopy. It crystallizes in the tetragonal space group  $P4_322$  (No. 95) with  $a = 7.3431(2)$  Å,  $c = 38.911(3)$  Å, and  $Z = 8$ . Its structure contains tetrameric units of the composition  $\text{Nb}_4\text{O}_{18}$ , which share corners to form a layer of niobium oxide. The Nb–O layer is a slice of the pyrochlore structure. Neighboring Nb–O layers are linked by vierer single-ring silicates generating eight-ring and six-ring channels running parallel to  $\langle 100 \rangle$  directions, in which the  $\text{Rb}^+$  cations and water molecules reside. The tantalum analogue was prepared and characterized by powder X-ray diffraction. Upon heating to 500 °C,  $\text{Rb}_2(\text{Nb}_2\text{O}_4)(\text{Si}_2\text{O}_6) \cdot \text{H}_2\text{O}$  loses lattice water molecules, while the framework structure is retained to give the anhydrous compound  $\text{Rb}_2(\text{Nb}_2\text{O}_4)(\text{Si}_2\text{O}_6)$ , whose structure was also characterized by single-crystal X-ray diffraction. The dehydrated sample absorbs water reversibly, as indicated by powder X-ray diffraction.  $\text{Rb}_2(\text{Nb}_2\text{O}_4)(\text{Si}_2\text{O}_6)$  crystallizes in the tetragonal space group  $I4_1$  (No. 80) with  $a = 10.2395(6)$  Å,  $c = 38.832(3)$  Å, and  $Z = 16$ .

### Introduction

Recently, much work has focused on the synthesis of silicates of transition metals,<sup>1–8</sup> main group elements,<sup>9–13</sup> lanthanide elements,<sup>14–25</sup> and uranium.<sup>26–33</sup> In contrast to zeolites, which are built of  $[\text{SiO}_4]^{4-}$  and  $[\text{AlO}_4]^{5-}$  tetrahedra, these metal silicate frameworks contain metals of varied coordination geometries. Most of these metal silicates were prepared under mild hydrothermal conditions at 180–240 °C in Teflon-lined autoclaves. Some of them were synthesized by high-temperature, high-pressure hydrothermal reactions at 500–600 °C in gold ampoules. Flux-growth techniques have also been used in exploratory synthesis. Several salt-inclusion metal silicates hosting alkali-metal halides in the framework structures were reported.<sup>12,34–36</sup>

Metal silicates that contain transition metals in octahedral or distorted octahedral framework sites have attracted interest

because they usually show good thermal stability and other physical and catalytic properties introduced by the transition-metal centers.<sup>1</sup> A large number of silicates containing titanium, zirconium, and vanadium have been synthesized and structurally characterized. In contrast, analogous systems based on niobium as the octahedral component are relatively rare. Niobium and tantalum silicates have been studied by Raveau and co-workers,<sup>37,38</sup> who found two structural types,  $\text{A}_3\text{Ta}_6\text{Si}_4\text{O}_{26}$  ( $\text{A} = \text{Ba}, \text{Sr}$ ) and  $\text{K}_6\text{M}_6\text{Si}_4\text{O}_{26}$  ( $\text{M} = \text{Nb}, \text{Ta}$ ),

- (3) Wang, X.; Liu, L.; Jacobson, A. J. *J. Am. Chem. Soc.* **2002**, *124*, 7812.
- (4) Brandão, P.; Valente, A.; Philippou, A.; Ferreira, A.; Anderson, M. W.; Rocha, J. *Eur. J. Inorg. Chem.* **2003**, 1175.
- (5) Nyman, M.; Bonhomme, F.; Teter, D. M.; Maxwell, R. S.; Bu, B. X.; Wang, L. M.; Ewing, R. C.; Nenoff, T. M. *Chem. Mater.* **2000**, *12*, 3449.
- (6) Nyman, M.; Bonhomme, F.; Maxwell, R. S.; Nenoff, T. M. *Chem. Mater.* **2001**, *13*, 4603.
- (7) Francis, R. J.; Jacobson, A. J. *Angew. Chem., Int. Ed.* **2001**, *40*, 2879.
- (8) Kao, H.-M.; Lii, K.-H. *Inorg. Chem.* **2002**, *41*, 5644.
- (9) Ferreira, A.; Lin, Z.; Rocha, J.; Morais, C. M.; Lopes, M.; Fernandez, C. *Inorg. Chem.* **2001**, *40*, 3330.
- (10) Ferreira, A.; Lin, Z.; Soares, M. R.; Rocha, J. *Inorg. Chim. Acta* **2003**, *356*, 19.
- (11) Hung, L.-I.; Wang, S.-L.; Chen, C.-Y.; Chang, B.-C.; Lii, K.-H. *Inorg. Chem.* **2005**, *44*, 2992.
- (12) Liao, C.-H.; Chang, P.-C.; Kao, H.-M.; Lii, K.-H. *Inorg. Chem.* **2005**, *44*, 9335.

\* Author to whom correspondence should be addressed. E-mail: liikh@cc.ncu.edu.tw.

<sup>†</sup> National Central University.

<sup>‡</sup> National Synchrotron Radiation Research Center.

<sup>§</sup> Academia Sinica.

(1) Rocha, J.; Anderson, M. W. *Eur. J. Inorg. Chem.* **2000**, 801.

(2) Wang, X.; Liu, L.; Jacobson, A. J. *Angew. Chem., Int. Ed.* **2001**, *40*, 2174.

which were prepared by high-temperature solid-state reaction. Three niobium silicate frameworks containing a novel silicate unit,  $\text{Si}_8\text{O}_{22}^{12-}$ , were synthesized under mild hydrothermal conditions by Salvadó et al.<sup>39</sup> We synthesized  $\text{Rb}_4(\text{NbO})_2(\text{Si}_8\text{O}_{21})$  under high-temperature, high-pressure hydrothermal conditions.<sup>8</sup> It is isotopic to  $\text{Cs}_4(\text{NbO})_2(\text{Si}_8\text{O}_{21})$ , which was prepared by solid-state reaction at 1100 °C by Crosnier et al.<sup>40</sup> The  $^{29}\text{Si}$  MAS NMR spectrum of  $\text{Rb}_4(\text{NbO})_2(\text{Si}_8\text{O}_{21})$  shows multiplet patterns which arise from  $^{93}\text{Nb}$  (spin-9/2)— $^{29}\text{Si}$   $J$ -coupling. This is the first example of two-bond  $J$ -coupling between a quadrupolar nucleus and a spin-1/2 nucleus in the solid state. Rocha et al. reported a microporous sodium niobosilicate,<sup>41</sup> AM-11, which can dehydrate *tert*-butyl alcohol to isobutene with high activity and selectivity. The first organically templated niobium silicate or germanate phases, NSH-1 and NGH-1, were synthesized by Francis and Jacobson.<sup>7</sup> Their 3-D frameworks consist of a network of interconnecting six-ring and eight-ring channels. In this paper, we report one result of exploratory high-temperature, high-pressure hydrothermal synthesis in the Rb/Nb/Si/O/H<sub>2</sub>O system.  $\text{Rb}_2(\text{Nb}_2\text{O}_4)(\text{Si}_2\text{O}_6)\cdot\text{H}_2\text{O}$  adopts a new structure containing a 3-D network of  $\text{NbO}_6$  and  $\text{SiO}_4$  units, linked via Nb—O—Nb and Nb—O—Si bonds. Its framework en-

closes an eight-ring channel, occupied by rubidium cations and water molecules. The tantalum analogue  $\text{Rb}_2(\text{Ta}_2\text{O}_4)(\text{Si}_2\text{O}_6)\cdot\text{H}_2\text{O}$  and the dehydrated phase of the niobium compound  $\text{Rb}_2(\text{Nb}_2\text{O}_4)(\text{Si}_2\text{O}_6)$  were also prepared and structurally characterized.

## Experimental Section

**Synthesis.**  $\text{Rb}_2(\text{Nb}_2\text{O}_4)(\text{Si}_2\text{O}_6)\cdot\text{H}_2\text{O}$  (denoted as **1**) was obtained from a high-temperature, high-pressure hydrothermal reaction in a gold ampule contained in a Leco Tem-Pres autoclave where pressure was provided by water. The apparatus is an externally heated cold-seal pressure vessel for use up to 10 000 bar and 750 °C. A reaction mixture of 260  $\mu\text{L}$  of  $\text{RbOH}(\text{aq})$  (50 wt %), 42 mg of  $\text{Nb}_2\text{O}_5$  (Acros, 99.5%), and 95 mg of  $\text{SiO}_2$  (Alfa Aesar, 99.995%) (molar ratio Rb/Nb/Si = 7:1:5) was loaded in a 4.3-cm-long gold ampule with an inside diameter of 4.8 mm. The open end of the ampule was crimped, hammered flat, and then welded with a torch. The sealed ampule was then placed in the autoclave and counter-pressured with water at a fill level of 55%. The autoclave was heated at 600 °C for 3 days and then cooled to 350 at 5 °C/h followed by quenching at room temperature by removing the autoclave from the tube furnace. The pressure at 600 °C was estimated to be 170 MPa according to the pressure—temperature diagram of pure water. The reaction produced colorless block crystals and colorless powder. The bulk product was pure, as indicated by powder X-ray diffraction (PXRD; Figure S1 in the Supporting Information). The yield was 86% based on niobium. Several crystals were selected for a single-crystal X-ray diffraction study, from which the chemical formula was determined to be  $\text{Rb}_2(\text{Nb}_2\text{O}_4)(\text{Si}_2\text{O}_6)\cdot\text{H}_2\text{O}$ . The thermogravimetric analysis (TGA) curve showed a weight loss of 3.29% in the range of 50–400 °C, which is close to the value of 3.05% calculated for the loss of one lattice water molecule (Figure S2 in the Supporting Information).

Upon heating to 500 °C, compound **1** loses lattice water molecules, while the framework structure remains to give the anhydrous compound  $\text{Rb}_2(\text{Nb}_2\text{O}_4)(\text{Si}_2\text{O}_6)$  (denoted as **2**). The crystal structures of **1** and **2** are closely related, but they crystallize in different space groups with different cell parameters. A dehydrated powder sample was exposed to moist air at room temperature, and its X-ray powder pattern was taken every several hours (Figure S3 in the Supporting Information). The results indicate that the dehydrated phase can absorb water reversibly.

The tantalum analogue  $\text{Rb}_2(\text{Ta}_2\text{O}_4)(\text{Si}_2\text{O}_6)\cdot\text{H}_2\text{O}$  was prepared by heating a reaction mixture of 232  $\mu\text{L}$  of  $\text{RbOH}(\text{aq})$  (Aldrich, 50 wt %), 62.3 mg of  $\text{Ta}_2\text{O}_5$  (Strem, 99.5%), and 84.7 mg of  $\text{SiO}_2$  (Alfa Aesar, 99.995%) (molar ratio Rb/Ta/Si = 7:1:5) in a 4.1-cm-long gold ampule under the same reaction conditions as those for **1**. The yield was 81% based on tantalum. The product was a colorless microcrystalline powder, and its X-ray powder pattern bore a close resemblance to that of **1**. The TGA curve showed a weight loss of 2.16% in the range of 50–600 °C, which is close to the value of 2.29% calculated for the loss of one lattice water molecule (Figure S4 in the Supporting Information). The sample was used for structure analysis by powder X-ray diffraction, as follows.

**Single-Crystal X-Ray Diffraction.** Most crystals of **1** in the reaction products were twinned. Many were selected and checked for reflection profiles before a satisfactory one was obtained. A crystal of **1** with dimensions 0.062 × 0.088 × 0.112 mm<sup>3</sup> was selected for indexing and intensity data collection on a Bruker CCD diffractometer. Intensity data were collected at room temperature in 1271 frames with  $\omega$  scans (width 0.30° per frame). The program SADABS was used for absorption correction ( $T_{\text{min}} = 0.773$ ,  $T_{\text{max}}$

- (13) Hung, L.-I.; Wang, S.-L.; Kao, H.-M.; Lii, K.-H. *Inorg. Chem.* **2007**, *46*, 3301.
- (14) Rocha, J.; Ferreira, P.; Carlos, L. D.; Ferreira, A. *Angew. Chem., Int. Ed.* **2000**, *39*, 3276.
- (15) Ananias, D.; Ferreira, A.; Rocha, J.; Ferreira, P.; Rainho, J. P.; Morais, C.; Carlos, L. D. *J. Am. Chem. Soc.* **2001**, *123*, 5735.
- (16) Ferreira, A.; Ananias, D.; Carlos, L. D.; Morais, C. M.; Rocha, J. *J. Am. Chem. Soc.* **2003**, *125*, 14573.
- (17) Ananias, D.; Kostova, M.; Almeida Paz, F. A.; Ferreira, A.; Carlos, L. D.; Klinowski, J.; Rocha, J. *J. Am. Chem. Soc.* **2004**, *126*, 10410.
- (18) Jeong, H.-K.; Chandrasekaran, A.; Tsapatsis, M. *Chem. Commun.* **2002**, 2398.
- (19) Haile, S. M.; Wuensch, B. J. *Acta Crystallogr., Sect. B* **2000**, *56*, 335.
- (20) Haile, S. M.; Wuensch, B. J. *Acta Crystallogr., Sect. B* **2000**, *56*, 349.
- (21) Kollitsch, U.; Tillmanns, E. *Mineral. Mag.* **2004**, *68*, 677.
- (22) Huang, M.-Y.; Chen, Y.-H.; Chang, B.-C.; Lii, K.-H. *Chem. Mater.* **2005**, *17*, 5743.
- (23) Wang, G.; Li, J.; Yu, J.; Chen, P.; Pan, Q.; Song, H.; Xu, R. *Chem. Mater.* **2006**, *18*, 5637.
- (24) Ananias, D.; Almeida Paz, F. A.; Carlos, L. D.; Geraldes, C. F. G. C.; Rocha, J. *Angew. Chem., Int. Ed.* **2006**, *4*, 5–7938.
- (25) Lee, C.-S.; Liao, Y.-C.; Hsu, J.-T.; Wang, S.-L.; Lii, K.-H. *Inorg. Chem.* **2008**, *47*, 1910.
- (26) Wang, X.; Huang, J.; Jacobson, A. J. *J. Am. Chem. Soc.* **2002**, *124*, 15190.
- (27) Huang, J.; Wang, X.; Jacobson, A. J. *J. Mater. Chem.* **2003**, *13*, 191.
- (28) Burns, P. C.; Olson, R. A.; Finch, R. J.; Hanchar, J. M.; Thibault, Y. *J. Nucl. Mater.* **2000**, *278*, 290.
- (29) Burns, P. C. *Can. Mineral.* **2005**, *43*, 1839.
- (30) Chen, C.-S.; Kao, H.-M.; Lii, K.-H. *Inorg. Chem.* **2005**, *44*, 935.
- (31) Chen, C.-S.; Chiang, R. K.; Kao, H.-M.; Lii, K.-H. *Inorg. Chem.* **2005**, *44*, 3914.
- (32) Chen, C.-S.; Lee, S.-F.; Lii, K.-H. *J. Am. Chem. Soc.* **2005**, *127*, 12208.
- (33) Lin, C.-H.; Chen, C.-S.; Shiryayev, A. A.; Zubavichus, Ya. V.; Lii, K.-H. *Inorg. Chem.* **2008**, *47*, 4445.
- (34) Schmidt, A.; Glaum, R. *Inorg. Chem.* **1997**, *36*, 4883.
- (35) Mo, X.; Hwu, S.-J. *Inorg. Chem.* **2003**, *42*, 3978.
- (36) Mo, X.; Ferguson, E.; Hwu, S.-J. *Inorg. Chem.* **2005**, *44*, 3121.
- (37) Choynet, J.; Nguyen, N.; Groult, D.; Raveau, B. *Mater. Res. Bull.* **1976**, *11*, 887.
- (38) Choynet, J.; Nguyen, N.; Raveau, B. *Mater. Res. Bull.* **1977**, *12*, 91.
- (39) Salvadó, M. A.; Pertierra, P.; Garcia-Granda, S.; Khainakov, S. A.; Garcia, J. R.; Bortun, A. I.; Clearfield, A. *Inorg. Chem.* **2001**, *40*, 4368.
- (40) Crosnier, M. P.; Guyomard, D.; Verbaere, A.; Piffard, Y. *Eur. J. Solid State Inorg. Chem.* **1990**, *27*, 435.
- (41) Rocha, J.; Brandão, P.; Philippou, A.; Anderson, M. W. *Chem. Commun.* **1998**, 2687.

= 0.947). On the basis of systematic absences, statistical analysis of intensity distribution, and successful solution and refinement of the structure, the space group was determined to be  $P4_322$  (No. 95). The structure was solved by direct methods and difference Fourier syntheses. The H atoms of the lattice water molecules were not located. Several O atoms were refined with isotropic thermal parameters because they gave nonpositive definite values when they were refined anisotropically. The final cycles of least-squares refinement including atomic coordinates for all atoms and anisotropic thermal parameters for most atoms converged at  $R_1 = 0.0304$  and  $wR_2 = 0.0692$ . The residual electron densities ( $\Delta\rho_{\max} = 1.93$ ,  $\Delta\rho_{\min} = -1.26 e \text{ \AA}^{-3}$ ) in the final difference Fourier maps were close to Rb atoms. The Flack parameter was 0.49(2), indicating the presence of inversion twinning in the crystal. ADDSYM detects additional symmetry elements. However, attempts to refine the structure in other possible space groups were unsuccessful.

A dehydrated crystal of **2** was covered with mineral oil to keep the crystals from moist air. A crystal with dimensions  $0.062 \times 0.112 \times 0.112 \text{ mm}^3$  was selected for indexing and intensity data collection on the same CCD diffractometer. The unit cell volume of **2** is nearly twice that of **1**. The program SADABS was also used for absorption correction ( $T_{\min} = 0.823$ ,  $T_{\max} = 0.949$ ). The space group was determined to be  $I4_1$  (No. 80). The Rb(6) and Rb(7) sites are partially occupied with an occupancy factor of 0.5. One O atom was refined with isotropic thermal parameters. The final cycles of least-squares refinement including atomic coordinates for all atoms and anisotropic thermal parameters for most atoms converged at  $R_1 = 0.0272$  and  $wR_2 = 0.0608$  ( $\Delta\rho_{\max} = 1.75$ ,  $\Delta\rho_{\min} = -1.53 e \text{ \AA}^{-3}$ ). The Flack parameter was 0.51(1). All calculations were performed using the SHELXTL version 5.1 software package.<sup>42</sup> ADDSYM detects additional symmetry elements and suggests a possible pseudo/new space group,  $I4_122$ . However, attempts to refine the structure in this new space group were unsuccessful.

**Powder X-Ray Diffraction.** PXRD measurements were performed at a wiggler beamline, BL17A, by using a triangular bent Si(111) monochromator of the National Synchrotron Radiation Research Center (NSRRC) in Taiwan. PXRD patterns were collected on compound **3** using an imaging plate (Fuji BAS; area =  $20 \times 40 \text{ cm}^2$ ) with a wavelength of  $1.3344 \text{ \AA}$  and a typical exposure time of  $\sim 5 \text{ min}$ . One-dimensional intensity profiles were obtained from an integration of the two-dimensional Debye–Scherrer rings by using the FIT2D program for better data statistics. The diffraction angle was calibrated by a mixture of silver behenate and silicon powder. It was possible to completely index the Bragg peaks in the pattern. The tetragonal unit cell obtained ( $a = 7.3820(1) \text{ \AA}$ ,  $c = 39.4613(7) \text{ \AA}$ ) and the diffraction pattern itself indicate that compound **3** is isostructural with **1**. Structural refinements were made by using the GSAS program<sup>43</sup> based on the structure model of  $\text{Rb}_2(\text{Nb}_2\text{O}_4)(\text{Si}_2\text{O}_6) \cdot \text{H}_2\text{O}$  determined from the single-crystal X-ray diffraction. Positional parameters and isotropic thermal parameters were refined. The final cycle of refinement converged to  $R_p = 0.0737$  and  $R_{wp} = 0.1039$ , indicating good agreement between the observed and calculated intensities. The final Rietveld fit is shown in Figure 1.

**Solid-State NMR Measurements.** Solid-state  $^{29}\text{Si}$  NMR experiments were performed on a Varian Infinityplus-500 spectrometer, equipped with a Chemagnetics 7.5 mm magic angle spinning (MAS) probe, with a resonance frequency of 99.3 MHz for the  $^{29}\text{Si}$  nucleus.

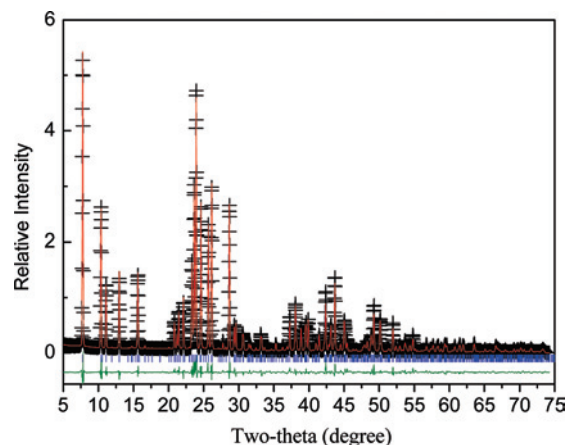


**Figure 1.** Final Rietveld profile ( $\lambda = 1.3344 \text{ \AA}$ ) of the synchrotron X-ray powder data collected on compound **3** with experimental data (top), positions of Bragg reflections (middle), and difference plot (bottom).

**Table 1.** Crystallographic Data for  $\text{Rb}_2(\text{Nb}_2\text{O}_4)(\text{Si}_2\text{O}_6) \cdot \text{H}_2\text{O}$  (**1**) and  $\text{Rb}_2(\text{Nb}_2\text{O}_4)(\text{Si}_2\text{O}_6)$  (**2**)

compound	<b>1</b>	<b>2</b>
empirical formula	$\text{H}_2\text{Nb}_2\text{O}_{11}\text{Rb}_2\text{Si}_2$	$\text{Nb}_2\text{O}_{10}\text{Rb}_2\text{Si}_2$
$a/\text{\AA}$	7.3431(3)	10.2395(6)
$c/\text{\AA}$	38.911(3)	38.832(3)
$V/\text{\AA}^3$	2098.1(2)	4071.4(7)
Z	8	16
fw	590.96	572.94
space group	$P4_322$ (No. 95)	$I4_1$ (No. 80)
T, °C	23	23
$\lambda(\text{Mo K}\alpha)$ , \AA	0.71073	0.71073
$D_{\text{calcd}}$ , $\text{g}\cdot\text{cm}^{-3}$	3.742	3.739
$\mu(\text{Mo K}\alpha)$ , $\text{cm}^{-1}$	116.8	120.3
$R_1^a$	0.0304	0.0272
$wR_2^b$	0.0692	0.0608

<sup>a</sup>  $R_1 = \sum ||F_o| - |F_c|| / \sum |F_o|$ . <sup>b</sup>  $wR_2 = [\sum w(F_o^2 - F_c^2)^2 / \sum w(F_o^2)^2]^{1/2}$ ,  $w = 1/[\sigma^2(F_o^2) + (aP)^2 + bP]$ ,  $P = [\text{Max}(F_o^2, 0) + 2(F_c^2)^2]/3$ , where  $a = 0.0184$  and  $b = 16.07$  for **1** and  $a = 0.0198$  and  $b = 21.45$  for **2**.

A pulse length of  $2 \mu\text{s}$  ( $\pi/4$  pulse) and a repetition time of 50 s were used to obtain the  $^{29}\text{Si}$  MAS NMR spectrum. The  $^{29}\text{Si}$  chemical shift was externally referenced to tetramethylsilane at 0 ppm.

## Results and Discussion

**Structures.** The crystallographic data and selected bond lengths for **1** and **2** are given in Tables 1 and 2, respectively. The Rietveld structure refinement of the X-ray powder diffraction data of **3** (the Ta compound) shows that it is

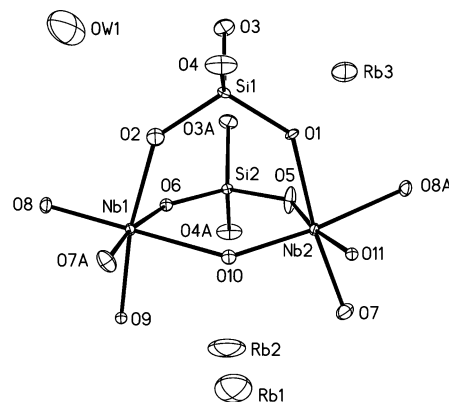


**Figure 2.** The asymmetric units of **1** showing the atom labeling scheme. Thermal ellipsoids are shown at 50% probability.

(42) Sheldrick, G. M. *SHELXTL*, version 5.1; Bruker AXS GmbH: Karlsruhe, Germany, 1998.

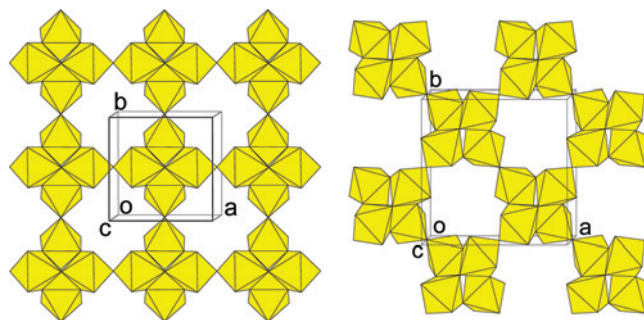
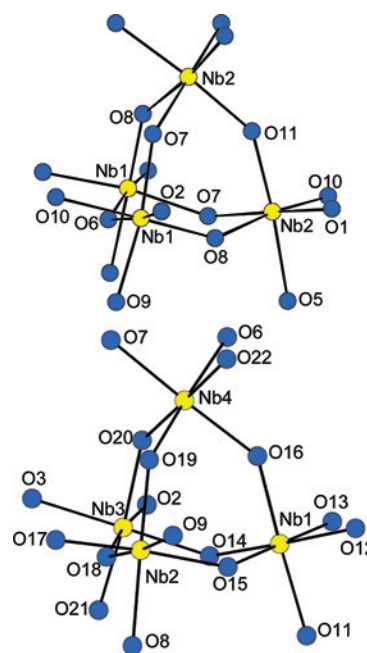
(43) Larson, A. C.; Von Dreele, R. B. *Generalized Structure Analysis System (GSAS)*; Report LAUR 86-748, Los Alamos National Laboratory: Los Alamos, NM, 1994.



**Table 2.** Selected Bond Lengths (Å) for  $\text{Rb}_2(\text{Nb}_2\text{O}_4)(\text{Si}_2\text{O}_6)\cdot\text{H}_2\text{O}$  (**1**) and  $\text{Rb}_2(\text{Nb}_2\text{O}_4)(\text{Si}_2\text{O}_6)$  (**2**)

Compound <b>1</b>			
Nb(1)–O(2)	2.022(6)	Nb(1)–O(6)	2.068(6)
Nb(1)–O(7)	1.941(5)	Nb(1)–O(8)	1.836(4)
Nb(1)–O(9)	1.953(3)	Nb(1)–O(10)	2.089(4)
Nb(2)–O(1)	2.066(5)	Nb(2)–O(5)	2.028(6)
Nb(2)–O(7)	1.939(4)	Nb(2)–O(8)	2.096(4)
Nb(2)–O(10)	1.821(4)	Nb(2)–O(11)	1.942(2)
Si(1)–O(1)	1.572(6)	Si(1)–O(2)	1.647(6)
Si(1)–O(3)	1.620(4)	Si(1)–O(4)	1.627(4)
Si(2)–O(3)	1.609(4)	Si(2)–O(4)	1.625(4)
Si(2)–O(5)	1.635(6)	Si(2)–O(6)	1.574(6)
Compound <b>2</b>			
Nb(1)–O(11)	2.018(4)	Nb(1)–O(12)	2.028(4)
Nb(1)–O(13)	1.917(4)	Nb(1)–O(14)	1.944(6)
Nb(1)–O(15)	1.946(4)	Nb(1)–O(16)	1.925(6)
Nb(2)–O(8)	2.034(4)	Nb(2)–O(9)	2.057(4)
Nb(2)–O(15)	1.956(4)	Nb(2)–O(17)	1.918(4)
Nb(2)–O(18)	1.943(5)	Nb(2)–O(19)	1.941(6)
Nb(3)–O(2)	2.071(4)	Nb(3)–O(3)	2.036(4)
Nb(3)–O(14)	1.947(6)	Nb(3)–O(18)	1.956(6)
Nb(3)–O(20)	1.945(4)	Nb(3)–O(21)	1.938(4)
Nb(4)–O(6)	2.031(4)	Nb(4)–O(7)	2.016(4)
Nb(4)–O(16)	1.945(6)	Nb(4)–O(19)	1.947(6)
Nb(4)–O(20)	1.942(4)	Nb(4)–O(22)	1.935(4)

isostructural with **1**. The covalent frameworks,  $\text{Rb}^+$  cations, and lattice water sites are essentially the same in both cases. In the following, only the structure of **1** is discussed. The asymmetric units for **1** are shown in Figure 2. The structure is constructed from the following building units: two  $\text{NbO}_6$  octahedra, two  $\text{SiO}_4$  tetrahedra, three Rb atoms, and one lattice water molecule. All atoms are in general positions except that Rb(2), Rb(3), and O(11) sit on 2-fold rotation axes. The observed Si–O bond lengths (1.572(6)–1.647(6) Å) and O–Si–O bond angles (106.7(3)–113.3(2)°) are typical values and are within the normal range.  $\text{SiO}_4$  tetrahedra are linked via two vertices to form four-membered single rings, corresponding to the composition  $[\text{SiO}_{2/2}\text{O}_{2/1}]_4$  or  $\text{Si}_4\text{O}_{12}$ . The bond angles at the bridging atoms O(3) and O(4) are 165.4(3)° and 156.2(2)°, respectively. Both Nb(1) $\text{O}_6$  and Nb(2) $\text{O}_6$  octahedra are distorted with the Nb–O bond lengths ranging from 1.836(4) Å to 2.089(4) Å for Nb(1) and 1.821(4) Å to 2.096(4) Å for Nb(2). The bond-valence sums are 5.06 and 5.13 for Nb(1) and Nb(2),<sup>44</sup> respectively, in accord with the occurrence of  $\text{Nb}^{5+}$  at these sites. Every  $\text{NbO}_6$  octahedron has two trans oxygen atoms that act as common vertices to other octahedra, forming orthogonal infinite zigzag chains parallel to  $\langle 100 \rangle$  directions. The bond angles at the bridging atoms O(8) and O(10) are 135.7(2)° and 143.2(2)°, respectively. The trans-metal–oxygen bond lengths are unequal. For each Nb atom, there is a short (ca. 1.82 Å) Nb–O bond trans to a long (ca. 2.08 Å) Nb–O bond. Each  $\text{NbO}_6$  octahedron within an infinite chain shares two cis equatorial oxygen atoms with two  $\text{NbO}_6$  octahedra in an adjacent orthogonal chain such that layers of niobium oxide in the  $ab$  plane with the composition  $\text{NbO}_{2/2}\text{O}_{2/2}\text{O}_{2/1}$ , that is,  $\text{NbO}_4$ , are formed (Figure 3). An alternative way to describe the structure is that it consists of a cluster of four  $\text{NbO}_6$  octahedra, each sharing three vertices, with the composition  $\text{Nb}_4\text{O}_{18}$  (Figure 4). Each cluster shares four

**Figure 3.** A Nb–O layer in **1** (left) and **2** (right).**Figure 4.** A tetrameric unit with the composition  $\text{Nb}_4\text{O}_{18}$  in **1** (top) and **2** (bottom).

vertices with four others to form a Nb–O layer with the composition  $\text{NbO}_4$ . Neighboring layers are linked by vierer single-ring silicates generating eight-ring and six-ring channels running parallel to  $\langle 100 \rangle$ , in which the  $\text{Rb}^+$  cations and water molecules reside (Figure 5). The longest and shortest  $\text{O}\cdots\text{O}$  distances across the eight-ring window are 7.34 and 5.64 Å, respectively. Using the maximum cation–anion distance of Donnay and Allmann,<sup>45</sup> a limit of 3.44 Å was set for Rb–O interactions, which gives the following coordination numbers: Rb(1), eight-coordinate; Rb(2), five-coordinate; Rb(3), 10-coordinate.

A tetrameric group of octahedra with  $T_d$  symmetry has been observed in  $\text{Te}_4\text{Cl}_{16}$ ,  $[\text{Pt}(\text{CH}_3)_3\text{Cl}]_4$ , and tungstates of the type  $\text{Li}_{14}(\text{WO}_4)_3\text{W}_4\text{O}_{16}\cdot 4\text{H}_2\text{O}$ .<sup>46</sup> Each octahedron shares three edges, and the four octahedra enclose a tetrahedral hole at the center. In contrast, each octahedron of the  $\text{Nb}_4\text{O}_{18}$  tetrameric group in **1** shares three corners, and the octahedra enclose an octahedral hole at the center. The  $\text{Nb}_4\text{O}_{18}$  unit of **1** has been observed in compounds with the pyrochlore

(45) Donnay, G.; Allmann, R. *Am. Mineral.* **1970**, *55*, 1003.(46) Wells, A. F. In *Structural Inorganic Chemistry*; Clarendon Press: Oxford, U.K. 1984; pp 199–203.(44) Brown, I. D.; Altermatt, D. *Acta Crystallogr., Sect B* **1985**, *41*, 244.

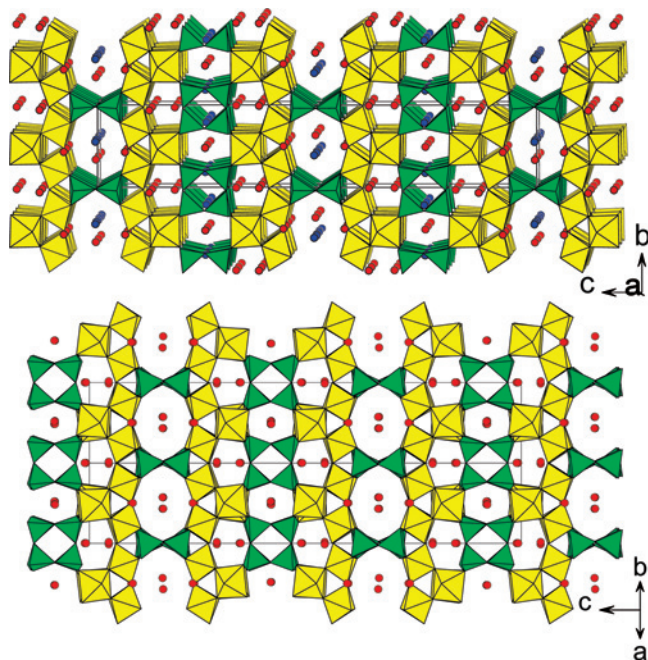


**Figure 5.** The structure of **1** and **2** viewed along the eight-ring channels. Yellow and green polyhedra represent  $\text{NbO}_6$  octahedra and  $\text{SiO}_4$  tetrahedra, respectively. Red circles,  $\text{Rb}^+$  cations; blue circles, water oxygen atoms.

structure such as  $\text{Cd}_2\text{Nb}_2\text{O}_7$ ,<sup>47</sup> and the Nb–O layer is a slice of the pyrochlore structure. The structure is named after the mineral pyrochlore, which has the approximate composition  $(\text{Ca},\text{Na})\text{Nb}_2\text{O}_6\text{F}$ .<sup>48</sup>

Compound **2** crystallizes in the tetragonal space group  $I4_1$  with a unit cell volume nearly twice that of compound **1**. The asymmetric unit for **2** consists of four  $\text{NbO}_6$  octahedra, four  $\text{SiO}_4$  tetrahedra, and seven  $\text{Rb}^+$  cation sites. All atoms are in general positions except that six  $\text{Rb}$ , O(17), O(21), and O(22) atoms sit on 2-fold rotation axes. In the structure of **2**, the lattice water molecule is removed from the eight-ring channels, and the neighboring  $\text{Nb}_4\text{O}_{18}$  units in the Nb–O layer are distinct, and therefore, the unit cell for **2** is twice the size of **1** (Figures 3 and 4). The two  $\text{Rb}^+$  cation sites in the eight-ring channels are 50% occupied. This dehydrated phase can absorb water reversibly, as indicated by powder X-ray diffraction.

**Solid-State NMR Spectroscopy.**  $^{29}\text{Si}$  solid-state NMR is used to provide information on the local environments of silicon atoms in the framework. The local environment of the  $\text{SiO}_4$  unit is sensitively reflected in the chemical shift of the central Si atom. In aluminosilicates, the replacement of one or more Si atoms by Al atoms results in significant low-field shifts. Si(1) and Si(2) both are  $\text{Q}^4(2\text{Nb})$  units. As shown in Figure 6, the  $^{29}\text{Si}$  spectrum of **1** shows a resonance at  $-95.9$  ppm, which is consistent with the observations that the chemical shifts of  $\text{Q}^4(2\text{Al})$  units in aluminosilicates are

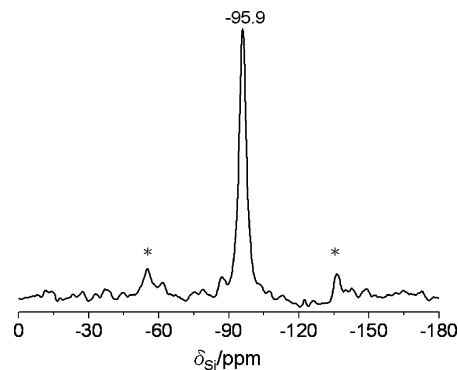


**Figure 6.**  $^{29}\text{Si}$  one-pulse MAS NMR spectrum of **1** acquired at a spinning speed of 4 kHz. Asterisks denote spinning sidebands.

in the range from  $-92$  to  $-99$  ppm,<sup>49</sup> and that of the  $\text{Q}^4(2\text{Nb})$  unit in  $\text{Rb}_4(\text{NbO})_2(\text{Si}_8\text{O}_{21})$  is  $-95$  ppm.<sup>8</sup> The spectral resolution is not high enough to distinguish the closely similar Si(1) and Si(2).

In summary, we have synthesized a new niobium(V) silicate,  $\text{Rb}_2(\text{Nb}_2\text{O}_4)(\text{Si}_2\text{O}_6)\cdot\text{H}_2\text{O}$ , by high-temperature, high-pressure hydrothermal methods and characterized the structure by single-crystal X-ray diffraction, TGA, and solid-state NMR spectroscopy. The 3-D framework structure contains layers of octahedral tetramers linked by rings of four  $\text{SiO}_4$  tetrahedra to generate eight-ring channels in which the  $\text{Rb}^+$  cations and water molecules reside. The Nb–O layer is a slice of the pyrochlore structure. The tantalum analogue  $\text{Rb}_2(\text{Ta}_2\text{O}_4)(\text{Si}_2\text{O}_6)\cdot\text{H}_2\text{O}$  was prepared and characterized by powder X-ray diffraction. Upon heating, the niobium compound loses lattice water molecules to give the anhydrous compound  $\text{Rb}_2(\text{Nb}_2\text{O}_4)(\text{Si}_2\text{O}_6)$ , which absorbs water reversibly. A single-crystal X-ray diffraction study of a dehydrated sample showed that the framework structure of the hydrate phase retains and transforms to a structure with a different space group and a unit cell volume about twice as big as the hydrate phase. Comparatively few studies are available on niobium silicates with open-framework structures. Niobium compounds have shown interesting catalytic properties when they are used as components of catalysts or when small amounts are added to known catalysts. Therefore, it would be particularly interesting to synthesize open-framework heterometal aluminosilicates with each metal occupying an individual site. Further work on this theme is in progress.

**Acknowledgment.** We thank the National Science Council for support and Prof. H.-M. Kao at National Central University for solid-state NMR measurements.

**Supporting Information Available:** Crystallographic data for **1** and **2** in CIF format, TGA curves, and X-ray powder patterns. This material is available free of charge via the Internet at <http://pubs.acs.org>.

IC801525D

(47) Brisse, F.; Stewart, D. J.; Seidl, V.; Knop, O. *Can. J. Chem.* **1972**, *50*, 3648.

(48) Wells, A. F. In *Structural Inorganic Chemistry*; Clarendon Press: Oxford, U.K. 1984; pp 604–605.

(49) Engelhardt, G.; Koller, H. In *Solid State NMR II, Inorganic Matter*; Blümich, B., Ed.; Springer Verlag: Berlin, 1994; pp 3–29.